

Phytochrome-Dependent Temperature Perception Modulates Isoprenoid Metabolism¹

Ricardo Bianchetti,^{a,2} Belen De Luca,^{b,2} Luis A. de Haro,^{b,3} Daniele Rosado,^{a,4} Diego Demarco,^a Mariana Conte,^c Luisa Bermudez,^{c,d} Luciano Freschi,^a Alisdair R. Fernie,^e Louise V. Michaelson,^f Richard P. Haslam,^f Magdalena Rossi,^{a,2} and Fernando Carrari^{b,d,2,5,6}

^aDepartamento de Botânica, Instituto de Biociências, Universidade de São Paulo, São Paulo 05508–090, Brazil

^bInstituto de Fisiología, Biología Molecular y Neurociencias, Consejo Nacional de Investigaciones Científicas y Técnicas, Ciudad Universitaria, C1428EHA Buenos Aires, Argentina

^cInstituto de Agrobiotecnología y Biología Molecular (IABIMO) INTA-CONICET (Instituto Nacional de Tecnología Agropecuaria). Hurlingham, 1686 Buenos Aires, Argentina.

^dCátedra de Genética, Facultad de Agronomía, Universidad de Buenos Aires, Buenos Aires C1417DSE, Argentina

^eMax Planck Institute of Molecular Plant Physiology, Potsdam-Golm D–14476, Germany

^fDepartment of Plant Sciences, Rothamsted Research, Harpenden, Hertshire AL5 2JQ, United Kingdom

ORCID IDs: 0000-0001-8739-5460 (R.B.); 0000-0003-0668-248X (L.A.d.H.); 0000-0002-9319-9041 (D.R.); 0000-0002-8244-2608 (D.D.); 0000-0001-9800-666X (M.C.); 0000-0002-9905-6287 (L.B.); 0000-0002-0737-3438 (L.F.); 0000-0001-9000-335X (A.R.F.); 0000-0001-5621-4495 (L.V.M.); 0000-0001-6226-5643 (R.P.H.); 0000-0003-3650-772X (M.R.); 0000-0003-0145-156X (F.C.)

Changes in environmental temperature influence many aspects of plant metabolism; however, the underlying regulatory mechanisms remain poorly understood. In addition to their role in light perception, phytochromes (PHYs) have been recently recognized as temperature sensors affecting plant growth. In particular, in *Arabidopsis* (*Arabidopsis thaliana*), high temperature reversibly inactivates PHYB, reducing photomorphogenesis-dependent responses. Here, we show the role of phytochrome-dependent temperature perception in modulating the accumulation of isoprenoid-derived compounds in tomato (*Solanum lycopersicum*) leaves and fruits. The growth of tomato plants under contrasting temperature regimes revealed that high temperatures resulted in coordinated up-regulation of chlorophyll catabolic genes, impairment of chloroplast biogenesis, and reduction of carotenoid synthesis in leaves in a PHYB1B2-dependent manner. Furthermore, by assessing a triple *phyAB1B2* mutant and fruit-specific *PHYA*- or *PHYB2*-silenced plants, we demonstrated that biosynthesis of the major tomato fruit carotenoid, lycopene, is sensitive to fruit-localized PHY-dependent temperature perception. The collected data provide compelling evidence concerning the impact of PHY-mediated temperature perception on plastid metabolism in both leaves and fruit, specifically on the accumulation of isoprenoid-derived compounds.

Temperature cues regulate plant primary and secondary metabolism, affecting several agronomically important traits in crop species (Suwa et al., 2010; Bitá and Gerats, 2013; Zhao et al., 2017). It has been established that heat disrupts chloroplast integrity, leading to further deficiencies of plastid-associated metabolites and a subsequent decline in plant performance (Yamori and von Caemmerer, 2009; Spicher et al., 2017). The ability to perceive stress conditions allows plants to adapt their metabolism in order to minimize any harmful effects on fitness (Saidi et al., 2011).

PHYTOCHROMES (PHYs) have been extensively described as light receptors. The biologically inactive PHY form (Pr) remains in the cytosol; however, once activated by red light, the active form (Pfr) is translocated toward the nucleus, where it assembles into photobodies and triggers photomorphogenesis-associated responses (Rockwell et al., 2006). The conversion of Pr to Pfr can be reversed by far-red light or darkness (Burgie and Vierstra, 2014). PHYB has been associated with a quantitative trait locus interval for thermoresponsive growth

in *Arabidopsis* (*Arabidopsis thaliana*; Box et al., 2015). High temperature (HT) reduces the abundance of Pfr by a quick and spontaneous reversion to Pr in a light-independent manner, consequently decreasing the size of nuclear bodies in a process termed thermoreversion (Legris et al., 2016). By contrast, lack of thermoreversion was detected in the hyperactive *phyB* mutant, resulting in the constitutive presence of photobodies regardless of temperature condition (Huang et al., 2019). As such, the *Arabidopsis phyB* null mutant mimics the transcriptional profile and physiological parameters of the wild-type counterpart grown under HT (Jung et al., 2016).

In tomato (*Solanum lycopersicum*), PHYs belong to a multigenic family encompassing five members: PHYA, PHYB1, PHYB2, PHYE, and PHYF (Alba et al., 2000b). We have previously demonstrated that PHYA, PHYB1, and PHYB2 positively control the biosynthesis of isoprenoid-derived compounds in tomato fruits in response to light (Bianchetti et al., 2018; Gramegna et al., 2019). PHYs posttranslationally down-regulate a group

of helix-loop-helix proteins named PHYTOCHROME INTERACTING FACTORS (PIFs; Park et al., 2018). PIFs derive from a multigenic family and have undergone subfunctionalization and neofunctionalization at the mRNA level (Rosado et al., 2016). It has been shown that SIPIF1a, SIPIF3, and SIPIF4 regulate carotenogenesis (Llorente et al., 2016), tocopherol biosynthesis (Gramegna et al., 2019), and sugar metabolism (Rosado et al., 2019), respectively, by light-dependent mechanisms.

Here, by analyzing the metabolic and transcriptional profiles of wild-type and *phy* mutant tomato plants grown under contrasting temperature conditions, we show that HT results in the reduction of leaf chlorophyll (Chl) and carotenoid levels in a PHYB1/B2-mediated manner through the regulation of Chl degradation and carotenoid biosynthetic genes, respectively. Furthermore, our data also demonstrate that HT or PHYB1B2 impairment leads to the transcriptional down-regulation of carotenoid biosynthetic genes in fruits, resulting in reduced levels of lycopene. Data obtained from fruit-specific *PHYA*- and *PHYB2*-silenced plants corroborated the role of fruit-localized PHYs in carotenoid accumulation through an intricate network in which master ripening transcription factors participate as mediators of temperature perception in tomato fruits.

¹This work was supported by the Sao Paulo Research Foundation (FAPESP; grant no. 2016/01128–9), CNPq, the Ministry of Science, Technology, and Innovation, Conselho Nacional de Desenvolvimento Científico e Tecnológico (grant no. 440976/2016–2), the European Research Council (grant no. 679796), and the Ministry of Science, Technology, and Productive Innovation, Argentina (grant no. 2014–0984 to F.C.). R.P.H. and L.V.M. were supported by the Biotechnology and Biological Sciences Research Council (grant no. BBS/E/C/00010420 to R.P.H.) and the United Kingdom-Brazil Alliance for Sustainable Agriculture scheme (grant no. BBS/OS/NW/000001). R.B. and D.R. were recipients of FAPESP fellowships (grant nos. 2017/24354–7 and 2015/14658–3). B.D.L. and L.A.d.H. are Consejo Nacional de Investigaciones Científicas y Técnicas (CONICET) fellows. L.B. and F.C. are members of CONICET. M.R. was a recipient of a CNPq fellowship.

²These authors contributed equally to the article.

³Present address: Department of Plant and Environmental Sciences, Weizmann Institute of Science, Rehovot 76100, Israel.

⁴Present address: Cold Spring Harbor Laboratory, Cold Spring Harbor, NY 11724.

⁵Senior author.

⁶Author for contact: fcarrari@fbmc.fcen.uba.ar.

The author responsible for distribution of materials integral to the findings presented in this article in accordance with the policy described in the Instructions for Authors (www.plantphysiol.org) is: Fernando Carrari (fcarrari@fbmc.fcen.uba.ar).

R.B. performed most of the experiments and analyzed the data; B.D.L. and L.A.d.H. performed experiments and analyzed data; D.R., D.D., and L.B. performed experiments; M.C., L.F., A.R.F., L.V.M., and R.P.H. contributed to experimental design and provided technical assistance; R.B., M.R., A.R.F., and F.C. conceived the project, designed experiments, and wrote the article, which was revised and approved by all authors.

www.plantphysiol.org/cgi/doi/10.1104/pp.20.00019

RESULTS

HT Affects the Plant Growth Phenotype in Tomato

To investigate the role played by PHYs in response to HT, 20-d-old plants from wild-type cv MoneyMaker (MM), *phyB1* and *phyB2* single mutants, and the *phyB1B2* double mutant were transferred to ambient temperature (AT; 24°C/18°C) and HT (30°C/24°C) growing conditions (Supplemental Fig. S1). Thirty days posttransfer, *phy* mutants displayed more elongated internodes than MM adult plants, as previously described (Kerckhoffs et al., 1997) under both temperature regimes, indicating that this is a genotype-dependent phenotype. On the other hand, for all the genotypes, HT promoted a narrower stem diameter, reduced leaf area, and less branching (Fig. 1A), exposing an HT-dependent phenotype. Thus, in these plants, no PHY-dependent HT phenotype was observed, which contrasted with that described in Arabidopsis seedlings, where HT increases elongation in a PHY-mediated manner (Jung et al., 2016). Moreover, no differences in relative water contents in leaves and fruits were observed between either genotypes or treatments (Supplemental Fig. S2). These results indicate that the applied temperature treatments affected plant growth without changing the water status of the plants, rendering the experimental setup suitable to study the impact of temperature on tomato metabolism in a PHY-dependent manner.

HT Alters Chlorophyll Metabolism and Fluorescence Parameters in a PHYB1/B2-Dependent Manner

Evidence about the role of PHYB in Chl biosynthesis (Inagaki et al., 2015) and its function as a thermosensor in Arabidopsis (Jung et al., 2016; Legris et al., 2017) led us to investigate the effects of PHYB1/B2-dependent temperature perception on tomato Chl metabolism. To address this question, Chl levels and fluorescence parameters were analyzed in leaves from 85-d-old plants of *phyB1*, *phyB2*, and *phyB1B2* mutants alongside the corresponding wild-type genotype. Notably, HT resulted in a significant reduction of total leaf Chl content in the MM genotype. However, the mutants were virtually insensitive to this temperature effect. Interestingly, regardless of the temperature treatment, leaf Chl content in the *phyB1B2* double mutant was the same as that observed in MM under HT (Fig. 1B). Additionally, under both temperature conditions, the *phyB1B2* double mutant, but not the *phyB1* and *phyB2* single mutants, exhibited values of light-adapted PSII maximum efficiency and PSII operating levels similar to those observed in MM under HT conditions and higher than MM under AT conditions. No impact of HT on dark-adapted PSII maximum quantum efficiency was observed in any genotype (Fig. 1C).

In order to gain insights into the regulatory role of PHYB1/B2 as temperature mediators in Chl metabolism, we further investigated the mRNA levels of genes

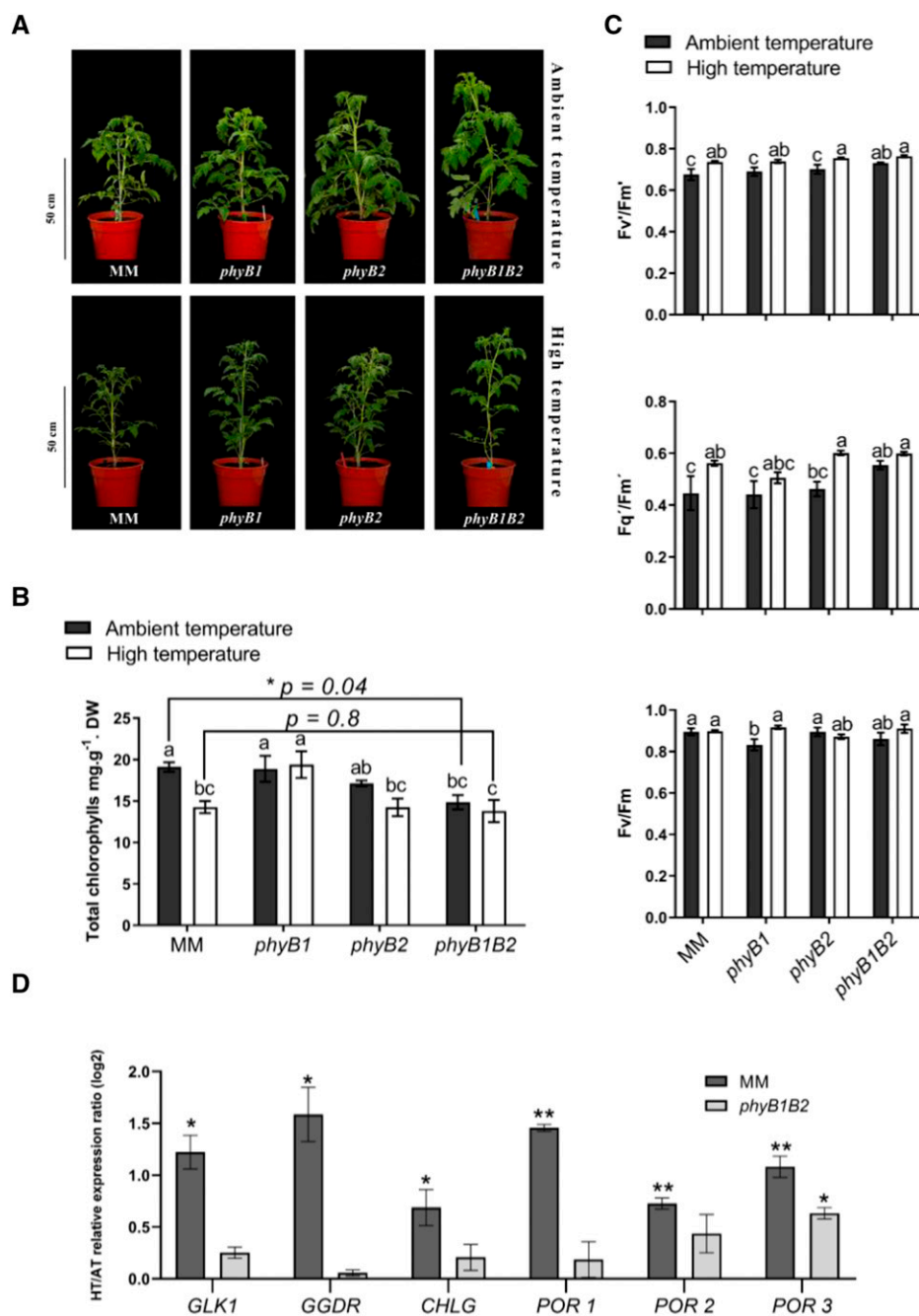


Figure 1. PHYB1/B2 are involved in temperature perception impacting leaf chlorophyll metabolism and fluorescence parameters in tomato. A, Side view of 50-d-old tomato MM plants and *phyB1*, *phyB2*, and *phyB1B2* knockout mutants grown under AT (day/night 24°C/18°C) and HT (day/night 30°C/24°C) conditions. B, Quantification of total Chl in the seventh fully expanded leaf from 85-d-old plants. Each bar represents the mean \pm SE. DW, Dry weight. C, PSII maximum efficiency (F_v'/F_m'), PSII operating efficiency (F_q'/F_m'), and maximum quantum efficiency of PSII (F_v/F_m') measured in the sixth fully expanded leaf from 85-d-old plants. n = at least five biological replicates. Each bar represents the mean \pm SE. In B and C, different letters indicate statistically significant differences according to Fisher's multiple comparison test ($P < 0.05$). Asterisk indicates statistically significant differences by two-tailed Student's t test ($P < 0.05$) between MM and *phyB1B2* under the same environmental conditions. D, HT/AT relative expression ratios of *GLK1*, *GGDR*, *CHLG*, *POR1*, *POR2*, and *POR3* mRNA abundance in MM and *phyB1B2* mutant leaf samples from 85-d-old plants. n = at least three biological replicates. Each bar represents the mean \pm SE. Asterisks (* $P < 0.05$ and ** $P < 0.01$) indicate statistically significant differences by two-tailed Student's t test between AT and HT within the same genotype. Gene abbreviations are defined in the text.

encoding key proteins involved in Chl biosynthesis that previously showed PHY-dependent transcriptional regulation (Gramegna et al., 2019; Alves et al., 2020). These genes included *GERANYLGERANYL DIPHOSPHATE REDUCTASE* (*GGDR*), the last enzyme for phytyl diphosphate chain synthesis (Almeida et al., 2015); the tetrapyrrole biosynthetic gene *PROTOCHLOROPHYLLIDE OXIDOREDUCTASE* (*POR*; three loci exist in the tomato genome named *POR1* [Solyc12g013710], *POR2* [Solyc10g006900], and *POR3* [Solyc07g054210], as revealed by the phylogenetic analyses presented in Supplemental Fig. S3); and *CHLOROPHYLL SYNTHASE* (*CHLG*), which condensates the tetrapyrrole ring with the phytyl

diphosphate (Almeida et al., 2015). Additionally, as a marker of chloroplast biogenesis and activity, we also included in the analysis the master transcriptional factor *GOLDEN2-LIKE1* (*GLK1*; Nguyen et al., 2014), which regulates the expression of Chl biosynthetic genes (Nakamura et al., 2009). HT resulted in significant increases in *GLK1*, *GGDR*, *CHLG*, *POR1*, *POR2*, and *POR3* mRNA levels in the leaves of the MM genotype, whereas the *phyB1B2* double mutant displayed a constitutive HT phenotype regarding the expression of Chl biosynthetic genes (except for the case of *POR3*; Fig. 1D; Supplemental Table S1), exposing a PHYB1/B2-dependent induction of Chl biosynthesis under HT conditions.

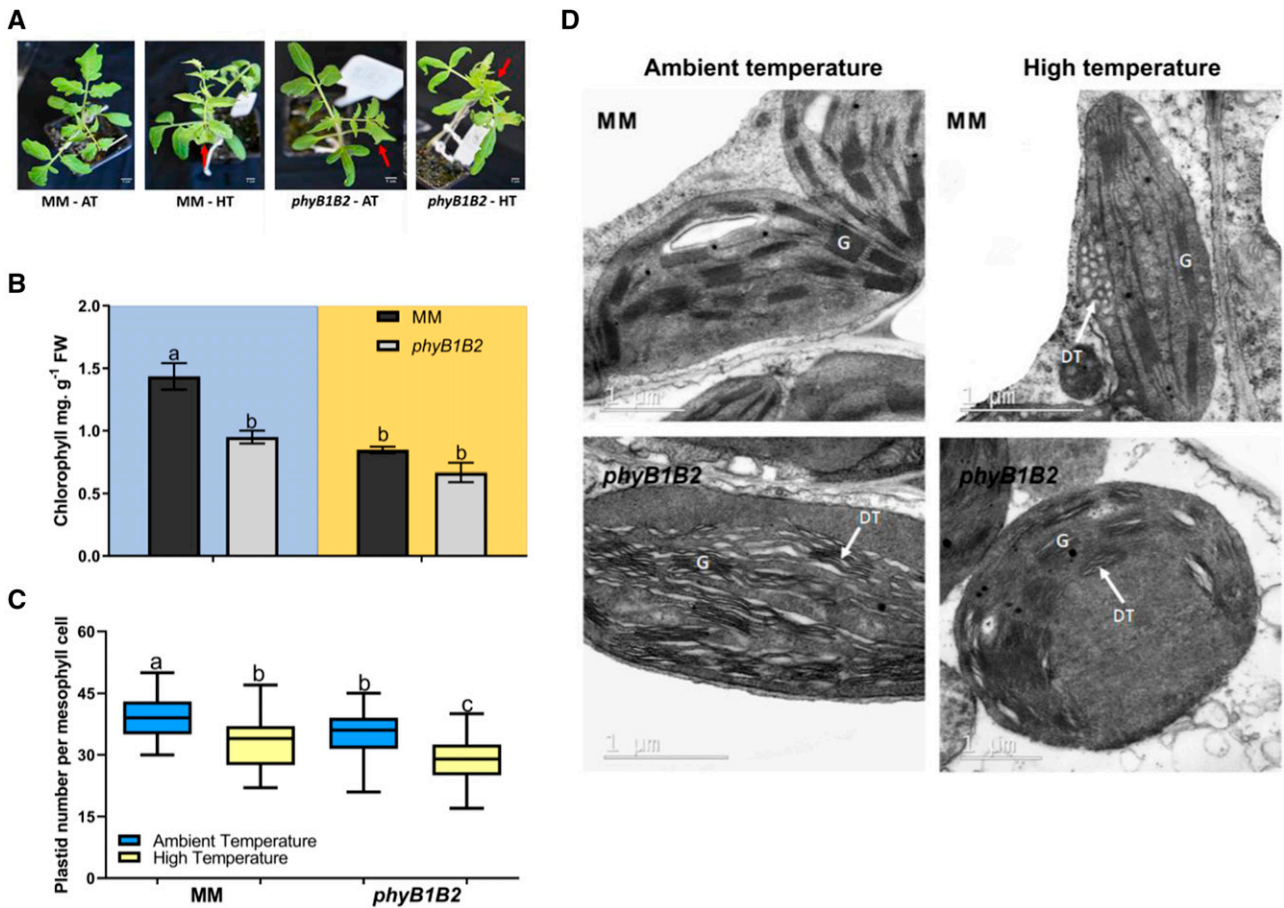


Figure 2. HT affects plastid biogenesis and development in leaves in a PHYB1/B2-dependent manner. **A**, Visualization of representative leaves from 21-d-old tomato MM and *phyB1B2* knockout mutants after 2 weeks under AT (day/night 24°C/18°C) and HT (30°C/24°C) conditions. Red arrows indicate chlorotic leaves (MM at HT, *phyB1B2* at AT, and *phyB1B2* at HT). **B**, Quantification of total Chl in leaves cultivated under AT (blue background) and HT (yellow background) conditions. *n* = at least three biological replicates. Each bar represents the mean ± SE. FW, Fresh weight. **C**, Plastid density per mesophyll cell. Values represent chloroplast quantification of ±70 cells. Each bar represents the mean ± SE. In **B** and **C**, different letters indicate statistically significant differences according to Fisher’s multiple comparison test (*P* < 0.05). **D**, Representative transmission electron microscopy images of chloroplasts from MM and *phyB1B2* leaves grown under AT and HT conditions. G indicates grana and DT indicates dilated thylakoids.

Taken together, these results show that Chl accumulation is regulated by temperature in a PHYB1/B2-dependent manner synergistically and reveal that temperature-induced Chl reduction is not the consequence of PHY-mediated impairment in Chl biosynthesis.

HT and PHYB1/B2 Deficiency Impact Chloroplast Biogenesis and Differentiation

The effect of PHYs (Oh and Montgomery, 2014; Martín et al., 2016) and temperature (Takahashi and Murata, 2008; van Eerden et al., 2015) on chloroplast biogenesis and structure have already been studied separately in several plant species. However, these two variables have not been previously assayed in an integrated manner in tomato, nor have they been assessed

in any other crop species where chloroplasts determine nutritional quality. Here, we evaluated whether the HT-induced impact on chloroplast development is mediated by PHYB1/B2 in tomato. Similar to that observed for 85-d-old plants (Fig. 1B), 21-d-old plants of MM, grown under HT conditions, and the *phyB1B2* mutant, regardless of the temperature condition, showed chlorotic symptoms (Fig. 2A, red arrows). This visual phenotypic difference agreed with lower measurements of leaf Chl content (Fig. 2B), strengthening the idea of PHYB1/B2 as a mediator of temperature perception modulating leaf Chl metabolism. Thus, to address whether differences in Chl levels were associated with changes in chloroplast biology, plastid quantification and ultrastructure analyses were performed in mesophyll cells. Microscopy data revealed a reduction in the number of chloroplasts per mesophyll cell in MM plants grown under HT and in the *phyB1B2*

double mutant cells under AT and HT compared with the MM genotype under AT (Fig. 2C). Interestingly, the *phyB1B2* double mutant still showed a slight temperature response, indicating the existence of PHY-independent temperature sensing, as reported in Arabidopsis (Ma et al., 2016; Fujii et al., 2017). Additionally, leaves developed under HT exhibited remarkable changes in chloroplast ultrastructure (Fig. 2D). Chloroplasts of MM developed under HT and those of the *phyB1B2* double mutant, under both temperature regimes, showed reduced grana stacking and dilated thylakoid lumen in comparison with MM under AT.

PIF transcription factors have been shown to mediate PHY-dependent temperature perception and, in particular, PIF1 and PIF3 have been shown to regulate chloroplast development in Arabidopsis (Stephenson et al., 2009; Kim et al., 2016). In tomato, PIF4 has been shown to participate in temperature-dependent seedling elongation (Rosado et al., 2019). Although PIF accumulation is mostly regulated posttranslationally, we found that *PIF1b* mRNA levels increase under HT in the MM genotype but the *phyB1B2* double mutant was insensitive (Supplemental Fig. S4A). We also identified significant up-regulation of *PIF3* mRNA in response to HT in MM and in the *phyB1B2* mutant regardless of temperature. These alterations in *PIF1b* and *PIF3* mRNA levels may explain, at least in part, the reduced number of plastids and their altered ultrastructure.

In conclusion, our data suggest that temperature perception mediated by PHYB1/B2 has an impact on chloroplast development that ultimately determines their structure and function.

PHYB1/B2 Inactivation Mediated by HT Enhances the Chlorophyll Degradation Pathway in Leaves

In Arabidopsis, PHYB regulates leaf senescence in response to light conditions through PIF4/PIF5, which in turn induce Chl breakdown (Sakuraba et al., 2014). However, it is unknown how PHYB-mediated temperature perception operates on Chl catabolism. The Chl degradation pathway operates in tomato leaves during senescence (Guyer et al., 2014; Lira et al., 2014), leading to phytol chain removal followed by the linearization of the tetrapyrrole ring involving several enzymatic steps (summarized in Fig. 3A; Hörtensteiner, 2013). In brief, Chl *a* is converted to an intermediate phytol-free chlorophyllide *a* or a magnesium-free pheophytin *a* form by CHLOROPHYLLASE (CLH) and STAY GREEN (SGR), respectively. Chlorophyllide *a* and pheophytin *a* are subsequently converted into pheophorbide *a* through dechelation, mediated by STAY GREEN-LIKE (SGR-like), and dephytylation, mediated by PHEOPHYTINASE (PPH), respectively. Finally, pheophorbide *a* is linearized by PHEOPHORBIDE A OXYGENASE (PAO) to yield a red Chl catabolite. To understand Chl reductions observed under HT and in the *phyB1B2* mutant, we therefore measured the mRNA levels of *CLH1*, *CLH2*, *CLH4*, *SGR*, *PPH*, *SGR-like*, and *PAO*.

mRNA levels of *CLH2*, *CLH4*, *PPH*, *SGR-like*, and *PAO* were at least twofold up-regulated in MM plants cultivated under HT (Fig. 3B). Consistent with our proposed role of PHYB1/B2 in temperature perception, regardless of the temperature condition, the *phyB1B2* double mutant showed mRNA levels similar to those observed in MM under HT for the *CLH4*, *PPH*, *SGR-like*, and *PAO* genes (Fig. 3). It has been reported that Chl degradation is triggered by dark-induced senescence and mediated by PHY perception and PIF signaling (Sakuraba et al., 2014). In particular, SGR and PAO enzyme-encoding genes are directly up-regulated by PIF4 and PIF5 in Arabidopsis (Song et al., 2014; Zhang et al., 2015). Even though the *PIF4* mRNA profile did not respond to temperature in our experiment (Supplemental Fig. S4A), we cannot formally rule out its involvement in the regulation of this process, considering that we were able to identify PIF-binding motifs in the four genes that showed PHYB1/B2-mediated temperature modulation, specifically *CLH4*, *PPH*, *SGR-like*, and *PAO* (Supplemental Fig. S4B). This observation suggests that the PHY-PIF module acts similarly in tomato and Arabidopsis.

Collectively, these results demonstrated that PHYB1/B2 represses Chl catabolism genes in a temperature-dependent manner in tomato leaves.

PHYB1/B2-Dependent Temperature Perception Regulates Leaf Carotenoid Biosynthesis at the Transcriptional Level

Alongside the induction of the Chl degradation pathway, the HT treatment and the *phyB1B2* double mutation resulted in over 30% reduction of total leaf carotenoids (Fig. 4A). To understand the molecular basis of this reduction, we analyzed the transcriptional profile of carotenoid biosynthetic enzyme-encoding genes. *GERANYLGERANYL DIPHOSPHATE SYNTHASE1* (*GGPS1*), which produces the carotenoid precursor geranylgeranyl diphosphate (Quadrona et al., 2013), was shown to be down-regulated both in response to HT and in the *phyB1B2* double mutant (Fig. 4B). By contrast, genes encoding carotenoid downstream enzymes, such as PHYTOENE SYNTHASE2 (*PSY2*), PHYTOENE DESATURASE (*PDS*), CHROMOPLAST-SPECIFIC LYCOPENE- β CYCLASE, and CHLOROPLAST-SPECIFIC LYCOPENE- β CYCLASE, did not show PHYB1/B2-mediated temperature modulation (Supplemental Fig. S5). Thus, the results presented above indicate that, in tomato leaves, the accumulation of chloroplast photosynthetic pigments is controlled through transcriptional adjustments of Chl degradation and carotenoid biosynthesis genes by the AT in a PHYB1/B2-dependent manner.

Fruit Carotenoid Contents Are Modulated by Temperature through PHYA and PHYB1/B2

A role for PHYs in tomato fruit carotenoid accumulation has long been proposed (Alba et al., 2000a; Gupta

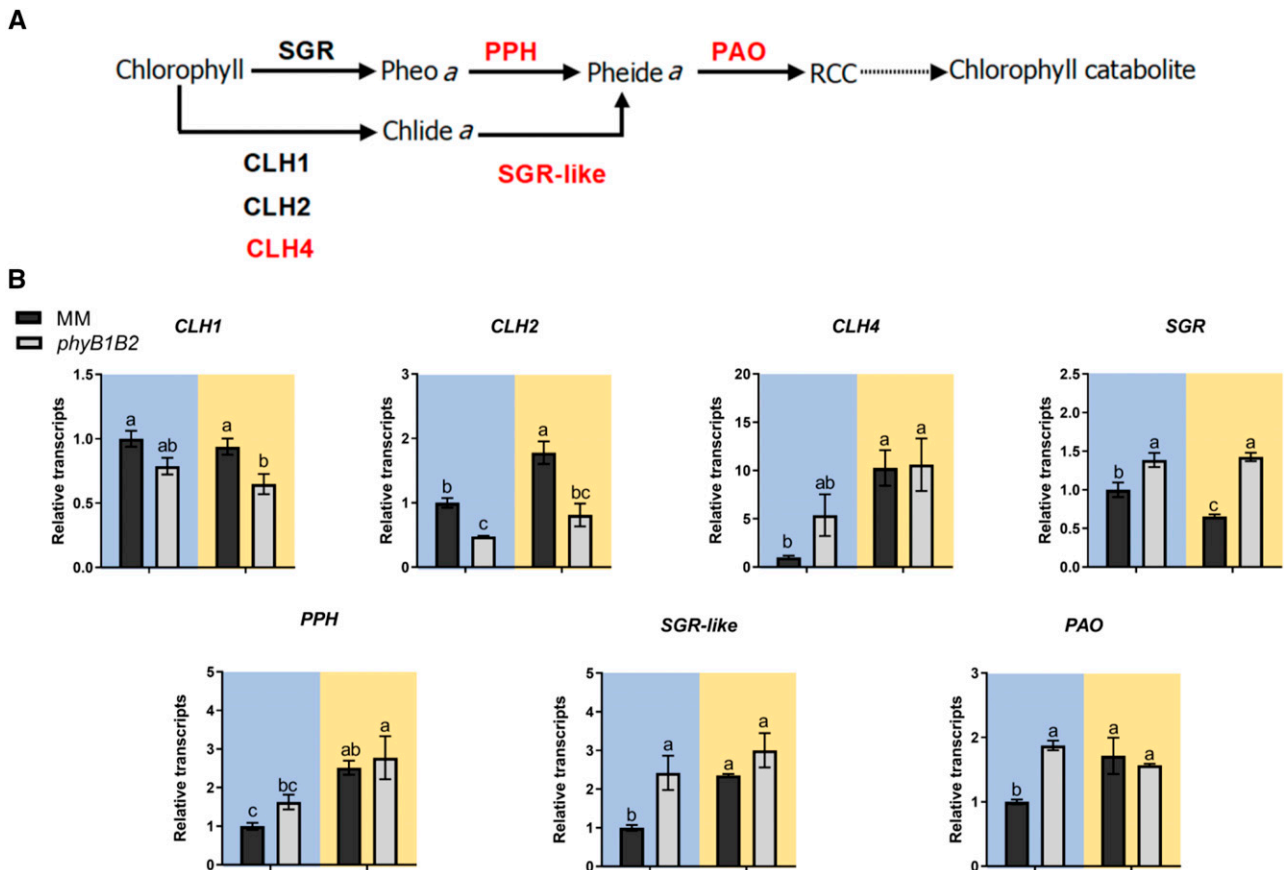


Figure 3. HT enhances chlorophyll degradation in leaves in a PHYB1/B2-dependent manner. A, Schematic model of the Chl degradation pathway. Enzymes and metabolites not defined in the text are denoted as follows: Chlide *a*, chlorophyllide *a*; Pheide *a*, pheophorbide *a*; Pheo *a*, pheophytin *a*; RCC, red chlorophyll catabolite. The enzymes highlighted in red are those shown to be regulated by temperature in a PHYB1/B2-dependent manner according to B. B, Relative mRNA levels of Chl-degrading enzyme-encoding genes in MM and *phyB1B2* mutant leaf samples from 85-d-old plants grown under AT (24°C/18°C; blue background) and HT (30°C/24°C; yellow background) conditions. Expression levels are relative to MM – AT conditions. *n* = at least three biological replicates. Each bar represents the mean ± SE. Different letters indicate statistically significant differences according to Fisher’s multiple comparison test (*P* < 0.05).

et al., 2014), and we recently demonstrated that fruit-localized PHYA and PHYB2 positively influence fruit carotenoid accumulation (Bianchetti et al., 2018). Aiming to evaluate the temperature effects on carotenogenesis, we followed two complementary approaches: (1) investigate the single *phyA*, *phyB1*, and *phyB2* mutants and the triple *phyAB1B2* mutant, and (2) analyze fruit-specific RNA interference (RNAi) *PHYA*- and *PHYB*-silenced lines in the cv Micro-Tom (MT) background (*PHYA*^{RNAi} and *PHYB2*^{RNAi}). This would allow us to unravel whether fruit-localized PHYs regulate carotenogenesis in a temperature-dependent manner in this organ and if this mechanism is genotype independent.

Except for the *phyAB1B2* triple mutant, ripe fruits harvested from HT-grown plants exhibited reductions in total carotenoid content compared with that in AT counterparts (Fig. 5A). Ripe fruits collected from single *phyA*, *phyB1*, and *phyB* mutant plants or double *phyB1B2* mutant plants grown under AT displayed

lower total carotenoid levels those that in MM counterparts. Interestingly, an enhanced reduction was observed in the *phyAB1B2* triple mutant, which displayed similar total fruit carotenoid levels under both temperature regimes (Fig. 5A). HPLC carotenoid profiling revealed that the accumulation of lycopene, alongside its precursors phytoene and phytofluene, was reduced by HT compared with AT in all genotypes aside from in the triple *phyAB1B2* mutant, which showed similar profiles of phytoene, phytofluene, and lycopene in fruits developed under both temperature regimes (Fig. 5B; Supplemental Fig. S6).

To investigate whether the temperature-mediated reduction in carotenoid content is a consequence of the transcriptional regulation of carotenoid biosynthetic genes, we further profiled *GGPS2*, *PSY1*, and *PDS* mRNA abundances in MM and the *phyAB1B2* triple mutant. In agreement with enhanced carotenoid biosynthesis during ripening, the three analyzed genes displayed a clear induction in MM under AT at the

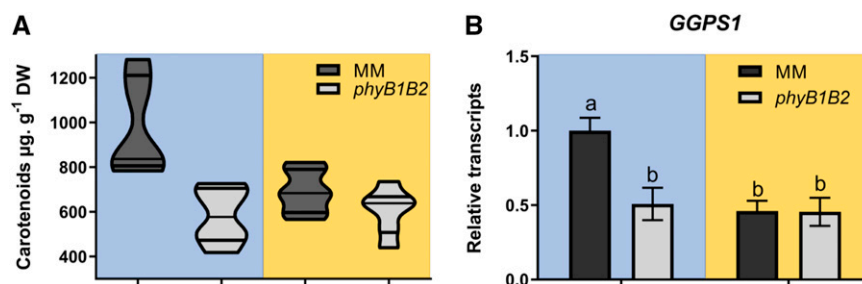


Figure 4. PHYB1/B2-dependent temperature perception transcriptionally regulates leaf carotenogenesis. A, Total carotenoid levels expressed in $\mu\text{g g}^{-1}$ dry weight (DW). $n =$ at least five biological replicates. B, Relative mRNA levels of *GGPS1* gene in MM and *phyB1B2* mutant leaf samples from 85-d-old plants grown under AT ($24^{\circ}\text{C}/18^{\circ}\text{C}$; blue background) and HT ($30^{\circ}\text{C}/24^{\circ}\text{C}$; yellow background) conditions. Expression levels are relative to MM–AT conditions. $n =$ at least three biological replicates. Each bar represents the mean \pm SE. Different letters indicate statistically significant differences according to Fisher's multiple comparison test ($P < 0.05$).

onset of ripening (from mature green to breaker stages). At the mature green stage, no significant difference in expression was observed attributable to genotype or temperature treatment. However, at the breaker stage, *GGPS2*, *PSY1*, and *PDS* mRNA levels were down-regulated in response to both temperature and the triple *phyAB1B2* mutation (Fig. 5B). The role of PIF1a in tomato fruit carotenogenesis has been previously reported. Although, upon induction of ripening, *PIF1a* transcript levels increased; concomitantly, Chl degradation alters the quality of the light filtered through the fruit pericarp, increasing the relative red/far-red light ratio. As a consequence, PIF degradation increases, enhancing *PSY1* expression and carotenoid accumulation (Llorente et al., 2016). Indeed, our results revealed PIF1a up-regulation from mature green to breaker stage in MM grown under AT, but its levels remained invariable in both genotypes under HT (Fig. 5C).

In summary, the temperature-insensitive phenotype observed in the *phyAB1B2* triple mutant fruits revealed that the inductive effect of PHYA/B1/B2 over the transcription of carotenogenesis-associated genes is abolished by HT conditions.

In order to mitigate the influence of any possible pleiotropic effect of *phy* mutations at the whole-plant level, we further analyzed fruit carotenoid accumulation in fruit-specific *PHYA*- and *PHYB2*-silenced lines, namely *PHYA*^{RNAi} and *PHYB2*^{RNAi}. Regardless of temperature, the lycopene content in *PHYA*^{RNAi} or *PHYB2*^{RNAi} fruit was reduced by half in comparison with control fruits developed under AT, the latter of which were affected by HT conditions (Fig. 6A). It is worth noting that this effect was observed in two independent transgenic lines for each genotype (Supplemental Fig. S7). In agreement, *PSY1* transcript accumulation accompanied the variations observed in lycopene content (Fig. 6B), confirming that fruit-localized PHY-mediated temperature perception controls carotenoid accumulation through transcriptional regulation of the biosynthetic enzyme-encoding genes.

PHYA- and PHYB2-Mediated Temperature Perception Controls Carotenoid Biosynthesis through Master Ripening Transcription Factors

Besides *PIF1a* (Llorente et al., 2016), *PSY1* expression has been demonstrated to be regulated by ripening-associated transcription factors in tomato (Liu et al., 2015). For this reason, we profiled the mRNA levels of candidate genes encoding master ripening regulators, namely *APETALA2a* (*AP2a*), *NON-RIPENING* (*NOR*), *RIPENING INHIBITOR* (*RIN*), *TOMATO AGAMOUS-LIKE* (*TAGL1*), and *FRUITFULL1* (*FUL1*) and *FUL2* (Klee and Giovannoni, 2011), in *PHY*^{RNAi} lines subjected to both temperature regimes.

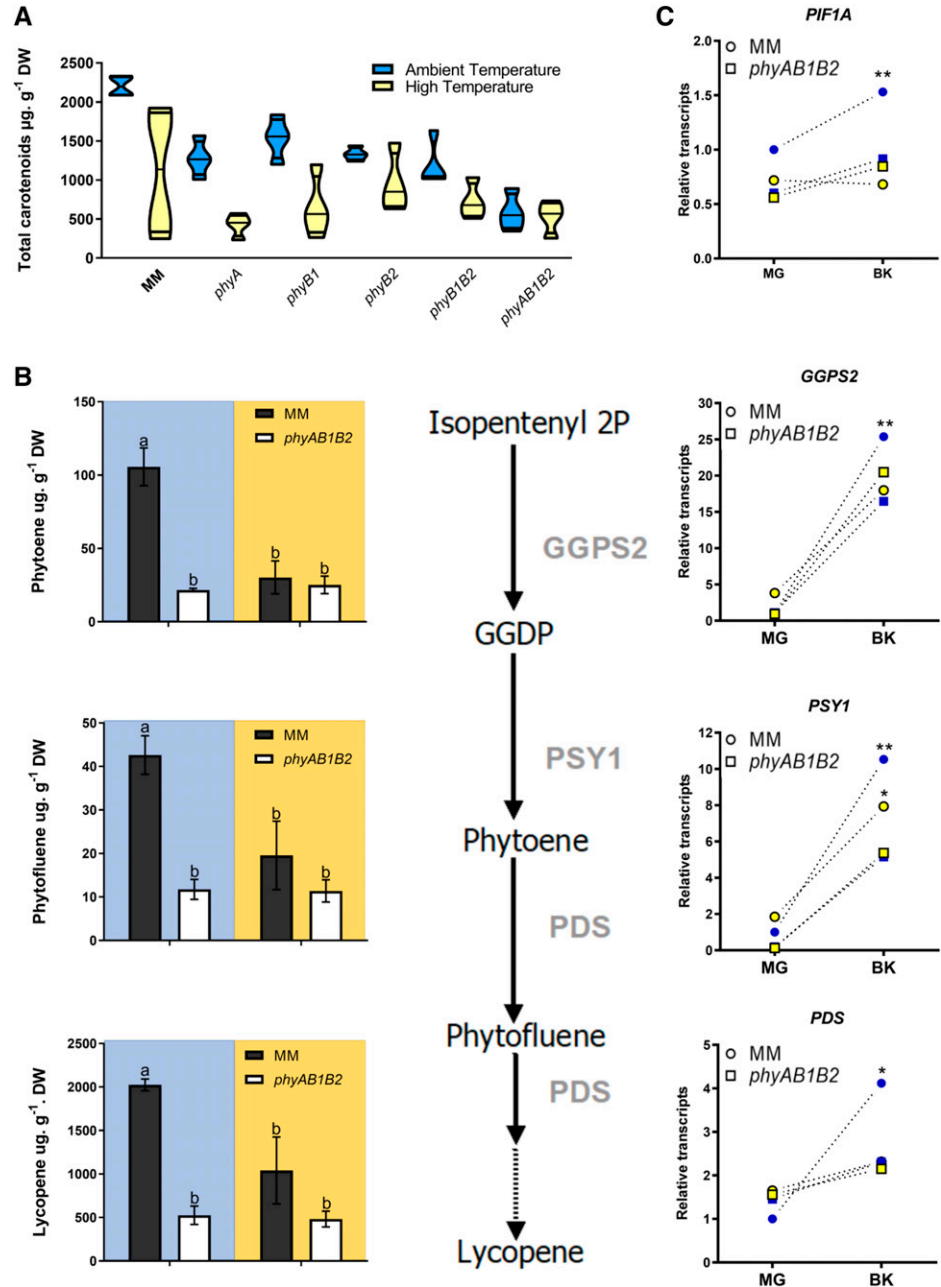
Three expression patterns were observed: (1) *RIN*, *TAGL1*, and *FUL1* mRNA levels responded to temperature treatment and in certain cases these responses varied in the absence of *PHYA* or *PHYB2*; (2) *FUL2* was down-regulated only in the lack of functional PHYs (*PHYA*^{RNAi} or *PHYB2*^{RNAi} lines); and (3) *AP2a* and *NOR* mRNAs displayed a clear response to PHY-mediated temperature perception (Fig. 6C). These results suggest that fruit-localized PHY-mediated temperature perception controls carotenoid accumulation via transcriptional regulation of ripening master controller genes.

Combined, these results decrypt the role of fruit-localized *PHYA* and *PHYB1/B2* as temperature sensors in tomato fruits, which regulate carotenoid accumulation through the transcriptional control of genes involved in their biosynthesis by alternative and converging molecular pathways.

DISCUSSION

Studies performed on plants under warm treatment or employing PHY signaling-defective mutants have demonstrated the synergistic influence of light and temperature on the regulation of chloroplast metabolism (Stephenson et al., 2009; Spicher et al., 2016, 2017; Zhao et al., 2016; Dubreuil et al., 2017). Despite this fact,

Figure 5. PHYA/B1/B2-dependent temperature perception transcriptionally regulates fruit carotenogenesis. **A**, Total carotenoid (phytoene, phytofluene, lycopene, lutein, and β -carotene) levels quantified from ripe fruits of MM and *phyA*, *phyB1*, *phyB2*, *phyB1B2*, and *phyAB1B2* mutant plants grown under AT (day/night 24°C/18°C; blue fill) and HT (day/night 30°C/24°C; yellow fill) conditions. **B**, Center, Schematic model of the lycopene biosynthetic pathway. The dotted line represents more than one enzymatic step. Left, Levels of lycopene, phytoene, and phytofluene in ripe fruits. AT, blue background; HT, yellow background. Each bar represents the mean \pm SE. Different letters indicate statistically significant differences according to Fisher's multiple comparison test ($P < 0.05$). DW, Dry weight. Right, Relative mRNA levels of carotenoid biosynthetic genes *GGPS2*, *PSY1*, and *PDS* in fruits at mature green (MG) and breaker (BK) stages harvested from plants grown under AT (blue) and HT (yellow) conditions. Transcript levels are expressed relative to MM MG – AT conditions. Asterisks ($*P < 0.05$ and $**P < 0.01$) indicate differences in the ANOVA in a multiple comparison test within the same fruit stage. **C**, Relative mRNA levels of the *PIF1a* carotenogenesis regulator gene in fruits at mature green and breaker stages harvested from plants grown under AT (blue) and HT (yellow) conditions. Transcript levels are expressed relative to MM MG – AT conditions. Asterisks ($**P < 0.01$) indicate differences in the ANOVA in a multiple comparison test within the same fruit stage.



the two factors have been studied independently, limiting our comprehensive understanding of light- and temperature-perception mechanisms at the molecular level. Recently, the role of PHYs as thermosensors by the gradual inactivation of PHYB by increasing temperature was reported in *Arabidopsis* (Legris et al., 2017). However, whether this mechanism operates in crop species evolved in different environments, and how this PHY-dependent temperature signaling cascade impacts major metabolic pathways, remain poorly understood. It is worth mentioning that PHY-independent temperature responses have also been described as associated with other photoreceptors (Ma et al., 2016; Fujii et al., 2017) and also in photoreceptor-impaired conditions

(Legris et al., 2016). In accordance, we also observed PHY-independent temperature responses here (Fig. 2C). In this study, we present experimental evidence that central enzyme-encoding genes of Chl and carotenoid metabolism are regulated at the transcriptional level by PHYB1/B2- and PHYA/B1/B2-mediated temperature perception in tomato leaf chloroplasts and fruit chloroplasts, respectively.

Constitutive HT-induced features were previously observed in the *Arabidopsis phyB* loss-of-function mutant (Jung et al., 2016; Huang et al., 2019). In contrast to the single-copy gene *PHYB* found in *Arabidopsis* (Sharrock and Quail, 1989), the tomato genome harbors two *PHYB* paralogs, *PHYB1* and *PHYB2*, which originated during a

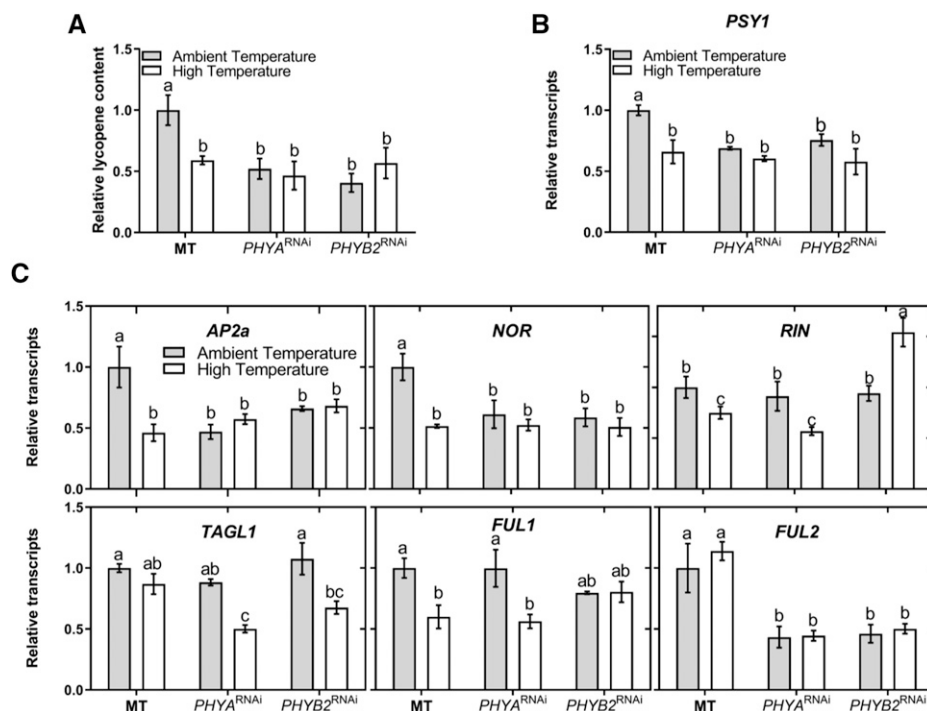


Figure 6. Fruit-localized PHYA and PHYB2 are involved in temperature perception impacting lycopene synthesis and master fruit-ripening regulators. A, Lycopene levels quantified in ripe fruits from MT control genotype and fruit-specific PHYA ($PHYA^{RNAi}$) and PHYB2 ($PHYB2^{RNAi}$) knockdown transgenic lines grown under AT (24°C/18°C) and HT (30°C/24°C) conditions. Lycopene levels were quantified and expressed relative to MT fruits under AT conditions, and values are means of at least three biological replicates from two independent lines for each genotype. Each bar represents the mean \pm SE. B and C, Relative mRNA levels of *PSY1* (B) and master fruit-ripening regulator genes (C) in MT, $PHYA^{RNAi}$, and $PHYB2^{RNAi}$ breaker fruit samples harvested under AT and HT conditions. Expression levels are relative to MT – AT conditions. $n =$ at least three biological replicates. Each bar represents the mean \pm SE. Different letters indicate statistically significant differences according to Fisher's multiple comparison test ($P < 0.05$).

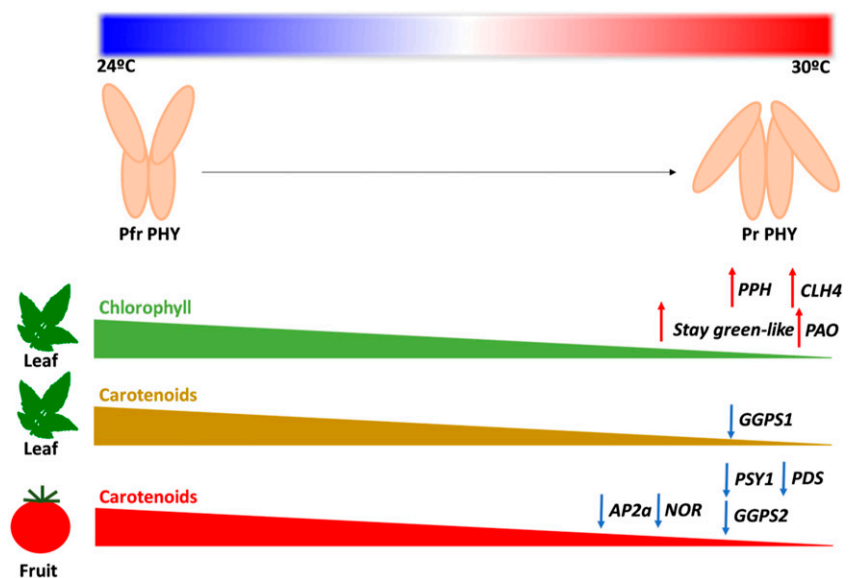
genome triplication event in the Solanaceae common ancestor (Tomato Genome Consortium, 2012). Indeed, results from this work indicate that loss of function in the double *phyB1B2* mutant, rather than single *phyB1* or *phyB2* mutation, is necessary to generate a thermoin-sensitive phenotype in tomato leaves leading to a reduction in Chl content, indicating that PHYB1 and PHYB2 play additive functions as temperature sensors (Fig. 1B). The *phyB1B2* double mutant did not show changes in the mRNA abundances of Chl biosynthetic genes in response to HT (Fig. 1D). However, these genes were up-regulated by HT in MM leaves, which does not explain the low-Chl phenotype shown by these plants (Fig. 1B) and suggests a highly complex regulatory mechanism.

Interestingly, together with the reduction in Chl content, increased Chl fluorescence parameters were registered (Fig. 1C). Our results are consistent with the finding in Arabidopsis that faster electron transport occurred under HT conditions, acting as an electron sink for the increment in photorespiration (Zhang and Sharkey, 2009).

The observable decrease in total Chl has been associated with a decrease in the LHCII, serving as a protective mechanism in plants undergoing abiotic stress

(Ishida et al., 2000). In agreement, we observed a reduction in chloroplast number and alterations in grana stacking (Fig. 2), probably mediated by higher *PIF3* mRNA level in response to PHYB1B2-mediated temperature inactivation (Supplemental Fig. S4A). In line with this, *PIF3* protein accumulation led to impaired chloroplast development in Arabidopsis (Stephenson et al., 2009). Moreover, our results provide genetic evidence that HT and the *phyB1B2* mutation trigger Chl catabolism via the up-regulation of genes associated with Chl degradation (i.e. *CLH4*, *PPH*, *SGR-like*, and *PAO*; Fig. 3). It was recently demonstrated that *PIF4* regulates senescence in tomato (Rosado et al., 2019). Additionally, PHYs trigger *PIF4* degradation (Lorrain et al., 2008), avoiding its inductive role in Chl breakdown (Sakuraba et al., 2014; Song et al., 2014; Zhang et al., 2015). In this sense, several canonical *PIF*-binding motifs, such as G- and PBE-box (Martínez-García et al., 2000; Zhang et al., 2013), were found in the promoter of the Chl-degrading-associated genes mentioned above (Supplemental Fig. S4B). Further reports extensively associate the inhibition of *PIF4* degradation in response to HT, impacting several events throughout the plant cycle (Koini et al., 2009; Qiu et al., 2019; Zhou et al., 2019). Together, these data suggest that inactivation

Figure 7. Effect of PHY-mediated temperature perception on tomato metabolism regulation. The rise of AT shifts the balance to the inactive Pr form, which promotes the Chl degradation pathway in source leaves through the transcriptional up-regulation of Chl catabolic enzyme-associated genes. Additionally, reduced levels of Pfr impair carotenoid accumulation in both leaves and ripe fruits, through the transcriptional down-regulation of carotenoid biosynthetic and master ripening regulator genes.



of PHYB1/B2 under HT affects Chl accumulation through altered chloroplast biogenesis (Fig. 2) and degradation (Fig. 3), likely via PIF1b/PIF3- and PIF4-dependent mechanism(s), respectively.

Our findings additionally indicate a down-regulation of *GGPS1* mRNA levels by temperature and the *phyB1B2* mutation (Fig. 4B). Since GGPS is the last shared step between the Chl and carotenoid biosynthetic pathways (Cordoba et al., 2009), this result is in accordance with the impairment of Chl and carotenoid synthesis in the leaves under these conditions (Figs. 2B and 4A).

Besides the impact on vegetative organs, our data also indicated that HT negatively influences carotenoid accumulation in tomato fruits (Fig. 5A). Alterations of isoprenoid-derived compounds in response to thermal stress have been increasingly demonstrated over the last years (Velikova et al., 2011; Spicher et al., 2016). Exposure of single, double, and triple PHY mutants as well as the MM control plants to two independent temperature regimes revealed a combinatory effect of temperature and the action of PHYs on carotenoid content of ripe fruits (Fig. 5A). In contrast to the other genotypes analyzed, the reduced levels of fruit lycopene and their precursors observed in *phyAB1B2* might be due to impaired temperature perception in this genotype (Fig. 5B). Consistent with this view, our findings indicate that the *phyAB1B2* mutations, as well as HT conditions, down-regulate the expression of the major carotenoid biosynthetic genes *GGPS2*, *PSY1*, and *PDS* (Fig. 5B). This is in agreement with our previous report showing that these genes are transcriptionally regulated by PHY-mediated light perception in tomato fruit (Bianchetti et al., 2018).

To further examine whether the observed impact on fruit carotenoids was the effect of whole-plant PHY deficiency or those localized in the fruits, we analyzed fruit-specific RNAi *PHYA*- and *PHYB*-silenced lines in

the MT genetic background (Bianchetti et al., 2018). The results showed equivalent reductions of lycopene accumulation and *PSY1* transcript levels in both transgenic lines, showing temperature insensitivity (Fig. 6, A and B), demonstrating that fruit-localized PHYs act as thermosensors and that this effect is genotype independent. Indeed, the central role played by temperature and PHYs controlling *PSY1* expression (Fig. 6B) is supported by previous studies demonstrating that PIF1a down-regulates carotenoid biosynthesis via *PSY1* transcriptional repression in tomato fruits (Llorente et al., 2016), similar to its ortholog in *Arabidopsis* in response to temperature (Toledo-Ortiz et al., 2014). In addition to PIF1a, carotenoid biosynthesis in tomato fruit is markedly regulated at the transcriptional level by the master ripening transcription factors *RIN*, *NOR*, *FUL1*, *FUL2*, *TAGL1*, and *AP2a* (Klee and Giovannoni, 2011). Whereas a noncombined effect of fruit-specific *PHY* expression and temperature on *RIN*, *TAGL1*, *FUL1*, or *FUL2* transcript abundance was observed, *AP2a* and *NOR* mRNA levels responded to temperature in a PHY-dependent manner (Fig. 6C), thus contributing to a reduction in lycopene content (Fig. 6A), most likely by the transcriptional regulation of *PSY1*, as previously described (Chung et al., 2010; Karlova et al., 2011; Yuan et al., 2016; Cruz et al., 2018). These results exposed an interesting network that regulates ripening in response to light and temperature in an independent or integrated way, warranting this key evolutionarily selected process.

Overall, our results support a model (Fig. 7) where increases in temperature induce the inactivation of PHYs, probably through the conformational change from the biologically active Pfr form to the inactive Pr form. The thermosensing role of PHYB1/B2 impacts leaf Chl and carotenoid levels through combined control of chloroplast biogenesis and the transcript levels of

carotenoid biosynthetic and Chl-degrading enzyme genes. Moreover, our data demonstrate that PHYA/PHYB1/PHYB2-mediated temperature perception modulates carotenoid metabolism in fruit. The data also showed the involvement of master ripening regulator genes as mediators of PHY-dependent temperature regulation of the carotenoid biosynthetic pathway. In conclusion, this study demonstrates the effect of PHY-mediated temperature perception on both photosynthetic and heterotrophic tomato plastid metabolism. Moreover, the results presented here identify the PHYs as critical hubs that can be manipulated to maintain and/or improve the nutritional quality of edible fruits in the context of global increasing temperatures.

MATERIALS AND METHODS

Plant Material, Growth Conditions, and Sampling

Tomato (*Solanum lycopersicum*) MM plants harboring loss-of-function mutations in *phyA*, *phyB1*, *phyB2*, *phyB1B2*, and *phyAB1B2* were previously characterized (Kerckhoffs et al., 1996, 1997, 1999; Lazarova et al., 1998a; 1998b; Weller et al., 2000). MT fruit-specific *PHYA*- and *PHYB2*-silenced lines (*PHYA*^{RNAi} and *PHYB2*^{RNAi}) were previously obtained and characterized by Bianchetti et al. (2018). Although MT is deficient in brassinosteroid biosynthesis due to the weak mutation *d*, it has been extensively demonstrated that it represents a convenient and adequate model system to study fruit biology (Campos et al., 2010). In this work, we used MT *PHYA*^{RNAi} and *PHYB2*^{RNAi} lines as a proof of concept that fruit-localized PHYs regulate carotenogenesis in a temperature-dependent manner in this organ and that this mechanism is genotype independent.

Tomato seeds (MM and MT) were sown under standard greenhouse conditions (day/night 24°C/18°C, 16/8 h light/dark, and 60% air relative humidity) in Floricultura Z substrate. Twenty-day-old plants were transplanted to 9-L pots and cultivated for 120 d (16/8 h light/dark and 60% air relative humidity) in greenhouses under two distinct temperature regimens: AT (24°C/18°C) and HT (30°C/24°C), with a mean daily difference of 5°C (Supplemental Fig. S1, A and B). These temperatures have been previously described as optimal and suboptimal highs for tomato (Ayenan et al., 2019). Plants were cultivated under 250 $\mu\text{mol m}^{-2} \text{s}^{-1}$ light intensity, which is lower than the tomato saturation point (approximately 800 $\mu\text{mol m}^{-2} \text{s}^{-1}$). To avoid unwanted effects on plant water status (Fahad et al., 2017), the plants were watered twice per day and the relative ambient humidity was monitored (Supplemental Fig. S1C). Leaves (seventh fully expanded leaf from bottom to top) and fruits (at mature green, breaker, and ripe [7 d after breaker] stages) from MM background plants were harvested 65 and 80 to 110 d after the beginning of the temperature treatment. Fruits from MT plants were harvested 75 to 90 d after the start of temperature treatment. Samples were ground in liquid N₂ and freeze dried prior to subsequent analysis.

Pigment Quantification

Chl extraction was carried out from 5 mg of freeze-dried leaf tissue in 1 mL of 80:20 acetone:Tris-HCl, 100 mM, pH 7.5. Samples were sonicated for 5 min at 42 kHz and further centrifuged at 16,000g for 2 min. The supernatant was collected, and the procedure was repeated until the green color was totally removed from the tissue. Spectrophotometer measurements were performed at 537, 647, 663, and 750 nm. Total Chl content was estimated by the following equation: $0.01373 \times (A663 - A750) - 0.000897 \times (A537 - A750) - 0.003046 \times (A647 - A750)$ (Sims and Gamon, 2003). For leaf carotenoid extraction, 5 mg of freeze-dried samples was immersed in 1 mL of *N,N*-dimethylformamide, sonicated for 5 min at 42 kHz, and centrifuged at 16,000g for 5 min. Supernatant absorbance was recorded at 480, 647, and 664 nm, then carotenoid contents were determined by the following equation: $[1,000 \times A480 - [1.12 \times (12 \times A664) - (3.11 \times A647)]] + [34.07 \times (20.78 \times A647) - (4.88 \times A664)] / 245$ (Wellburn, 1994). Fruit carotenoid extraction was carried out from 20 mg of freeze-dried fruit tissue according to Bianchetti et al. (2018). Phytoene,

phytofluene, lycopene, β -carotene, and lutein were determined by HPLC. Eluted compounds were detected at 450 nm (lycopene, β -carotene, and lutein), 286 nm (phytoene), and 347 nm (phytofluene) as described by Fraser et al. (2000).

Chl Fluorescence Measurements

Chl fluorescence parameters were determined according to Lira et al. (2017) using a portable open gas-exchange system (LI-6400XT system; LI-COR) equipped with an integrated modulated Chl fluorometer (LI-6400-40; LI-COR). Briefly, the second leaflet of the sixth fully expanded leaf from 85-d-old plants was kept under dark adaptation for 60 min, then weak and saturating white light pulses were applied to determine, respectively, initial fluorescence and maximum fluorescence emission. Furthermore, the same procedure was applied on light-adapted leaves to determine the light-adapted initial fluorescence and maximum fluorescence emission. The values were used to calculate maximum quantum efficiency of PSII, PSII operating efficiency, and PSII maximum efficiency.

Plastid Abundance and Ultrastructure

Two-week-old MM and *phyB1B2* plants grown under standard conditions were transferred to the distinct temperature conditions described above. After 1 week, the fourth fully expanded leaf was used to determine plastid abundance and for ultrastructure analysis.

Plastid abundance was determined in the leaf mesophyll as described by Bianchetti et al. (2017). In brief, leaf samples were incubated in 3.5% (v/v) glutaraldehyde for 60 min and then in 0.1 M Na-EDTA (pH 9.5) at 60°C for 180 min. Isolated cells were visualized through optical microscopy, and plastid number per cell was estimated using the ImageJ program (<https://imagej.nih.gov/ij/>).

For ultrastructure analysis, leaf segments were fixed at 4°C in Karnovsky's solution (2.5% [v/v] glutaraldehyde and 2% [v/v] paraformaldehyde in 0.1 M sodium phosphate buffer, pH 7.2) for 24 h. After washing in phosphate buffer, the samples were postfixed in buffered 1% (w/v) osmium tetroxide, washed, dehydrated in a graded series of acetone, and embedded in Spurr's resin. The resin was polymerized at 60°C. Ultrathin sections were stained with saturated uranyl acetate (Watson, 1958) and lead citrate (Reynolds, 1963) and observed using a JEM 1011 transmission electron microscope.

RNA Extraction and Reverse Transcription Quantitative PCR

RNA extraction, cDNA synthesis, primer design, and quantitative PCR (qPCR) assays were performed as described by Quadra et al. (2013). The primers used for reverse transcription qPCR analyses are listed in Supplemental Table S2. qPCR reactions were performed in a QStudio6-A1769 PCR Real-Time thermocycler using 2 \times Power SYBR Green Master Mix in a final volume of 10 μL . Absolute fluorescence data were analyzed using LinRegPCR software to obtain Ct and primer efficiency values. Relative mRNA abundance was calculated and normalized with the $\Delta\Delta\text{Ct}$ method using two reference genes (Expósito-Rodríguez et al., 2008): *EXPRESSED* and *TIP4.1* for leaves and *EXPRESSED* and *CAC* for fruits (Quadra et al., 2013).

Phylogenetic Analysis

Amino acid sequences of Arabidopsis (*Arabidopsis thaliana*) PORA, PORB, and PORC were BLASTed against the tomato genome in the Sol Genomics network database (<http://solgenomics.net>). Homologous sequences from tomato, Arabidopsis, *Arabidopsis lyrata*, *Brassica oleracea*, *Brassica rapa*, *Sorghum bicolor*, *Zea mays*, and *Setaria viridis* were retrieved by BLASTp against Viridiplantae in Phytozome (<http://phytozome.jgi.doe.gov/pz/portal.html>). The MUSCLE package available in MEGA software 10.0.3 (<https://www.megasoftware.net/>) was used to perform multiple sequence alignments. Phylogenetic reconstruction was performed with the maximum-likelihood method with 5,000 bootstrap replications.

Data Analysis

The values in the figures represent means of at least three biological replicates \pm SE. Statistical differences in parameters were analyzed with InfoStat/F

software (<http://www.infostat.com.ar>). Two-way ANOVA was performed to determine genotype (G), environment (E), or G×E interaction. Fisher's test ($P < 0.05$) was performed to compare G×E interaction, and Student's t test ($P < 0.05$) was applied to discriminate means of the sample within genotypes.

Accession Numbers

Sequence data from this article can be found in the GenBank/EMBL data libraries under accession numbers AJ001913 (*phyA*), AJ002281 (*phyB1*), and AF122901 (*phyB2*).

Supplemental Data

The following supplemental materials are available.

Supplemental Figure S1. Time course of temperature and relative humidity measurements registered along the plant growth cycle.

Supplemental Figure S2. Hydric status of MM and phytochrome knockout mutant plants at two temperatures regimes.

Supplemental Figure S3. Phylogenetic construction of the POR protein family.

Supplemental Figure S4. PIF involvement in the regulation of temperature-induced Chl reduction.

Supplemental Figure S5. Expression profile of carotenoid biosynthetic genes in leaves.

Supplemental Figure S6. Carotenoid profile in ripe fruits from MM and phytochrome knockout mutants.

Supplemental Figure S7. Lycopene content in ripe fruits from fruit-specific PHYA- and PHYB2-knockdown transgenic lines.

Supplemental Table S1. Relative expression of Chl biosynthetic genes.

Supplemental Table S2. Primer sequences used in this study.

Received February 4, 2020; accepted April 24, 2020; published May 14, 2020.

LITERATURE CITED

- Alba R, Cordonnier-Pratt MM, Pratt LH (2000a) Fruit-localized phytochromes regulate lycopene accumulation independently of ethylene production in tomato. *Plant Physiol* **123**: 363–370
- Alba R, Kelmenson PM, Cordonnier-Pratt MM, Pratt LH (2000b) The phytochrome gene family in tomato and the rapid differential evolution of this family in angiosperms. *Mol Biol Evol* **17**: 362–373
- Almeida J, Asís R, Molineri VN, Sestari I, Lira BS, Carrari F, Peres LEP, Rossi M (2015) Fruits from ripening impaired, chlorophyll degraded and jasmonate insensitive tomato mutants have altered tocopherol content and composition. *Phytochemistry* **111**: 72–83
- Alves FRR, Lira BS, Pikart FC, Monteiro SS, Furlan CM, Purgatto E, Pascoal GB, Andrade SCDS, Demarco D, et al (2020) Beyond the limits of photoperception: Constitutively active PHYTOCHROME B2 over-expression as a means of improving fruit nutritional quality in tomato. *Plant Biotechnol J* doi:10.1111/pbi.13362
- Ayenan MAT, Danquah A, Hanson P, Ampomah-Dwamena C, Sodedji FAK, Asante IK, Danquah EY (2019) Accelerating breeding for heat tolerance in tomato (*Solanum lycopersicum* L.): An integrated approach. *Agronomy (Basel)* **9**: 720
- Bianchetti RE, Cruz AB, Oliveira BS, Demarco D, Purgatto E, Peres LEP, Rossi M, Freschi L (2017) Phytochromobilin deficiency impairs sugar metabolism through the regulation of cytokinin and auxin signaling in tomato fruits. *Sci Rep* **7**: 7822
- Bianchetti RE, Silvestre Lira B, Santos Monteiro S, Demarco D, Purgatto E, Rothan C, Rossi M, Freschi L (2018) Fruit-localized phytochromes regulate plastid biogenesis, starch synthesis, and carotenoid metabolism in tomato. *J Exp Bot* **69**: 3573–3586
- Bitá CE, Gerats T (2013) Plant tolerance to high temperature in a changing environment: Scientific fundamentals and production of heat stress-tolerant crops. *Front Plant Sci* **4**: 273
- Box MS, Huang BE, Domijan M, Jaeger KE, Khattak AK, Yoo SJ, Sedivy EL, Jones DM, Hearn TJ, Webb AAR, et al (2015) ELF3 controls thermoresponsive growth in *Arabidopsis*. *Curr Biol* **25**: 194–199
- Burgie ES, Vierstra RD (2014) Phytochromes: An atomic perspective on photoactivation and signaling. *Plant Cell* **26**: 4568–4583
- Campos ML, Carvalho RF, Benedito VA, Peres LEP (2010) Small and remarkable: The Micro-Tom model system as a tool to discover novel hormonal functions and interactions. *Plant Signal Behav* **5**: 267–270
- Chung MY, Vrebalov J, Alba R, Lee J, McQuinn R, Chung JD, Klein P, Giovannoni J (2010) A tomato (*Solanum lycopersicum*) APETALA2/ERF gene, *SLAP2a*, is a negative regulator of fruit ripening. *Plant J* **64**: 936–947
- Cordoba E, Salmi M, León P (2009) Unravelling the regulatory mechanisms that modulate the MEP pathway in higher plants. *J Exp Bot* **60**: 2933–2943
- Cruz AB, Bianchetti RE, Alves FRR, Purgatto E, Peres LEP, Rossi M, Freschi L (2018) Light, ethylene and auxin signaling interaction regulates carotenoid biosynthesis during tomato fruit ripening. *Front Plant Sci* **9**: 1370
- Dubreuil C, Ji Y, Strand Å, Grönlund A (2017) A quantitative model of the phytochrome-PIF light signalling initiating chloroplast development. *Sci Rep* **7**: 13884
- Expósito-Rodríguez M, Borges AA, Borges-Pérez A, Pérez JA (2008) Selection of internal control genes for quantitative real-time RT-PCR studies during tomato development process. *BMC Plant Biol* **8**: 131
- Fahad S, Bajwa AA, Nazir U, Anjum SA, Farooq A, Zohaib A, Sadia S, Nasim W, Adkins S, Saud S, et al (2017) Crop production under drought and heat stress: Plant responses and management options. *Front Plant Sci* **8**: 1147
- Fraser PD, Pinto ME, Holloway DE, Bramley PM (2000) Application of high-performance liquid chromatography with photodiode array detection to the metabolic profiling of plant isoprenoids. *Plant J* **24**: 551–558
- Fujii Y, Tanaka H, Konno N, Ogasawara Y, Hamashima N, Tamura S, Hasegawa S, Hayasaki Y, Okajima K, Kodama Y (2017) Phototropin perceives temperature based on the lifetime of its photoactivated state. *Proc Natl Acad Sci USA* **114**: 9206–9211
- Gramegna G, Rosado D, Sánchez Carranza AP, Cruz AB, Simon-Moya M, Llorente B, Rodríguez-Concepción M, Freschi L, Rossi M (2019) PHYTOCHROME-INTERACTING FACTOR 3 mediates light-dependent induction of tocopherol biosynthesis during tomato fruit ripening. *Plant Cell Environ* **42**: 1328–1339
- Gupta SK, Sharma S, Santisree P, Kilambi HV, Appenroth K, Sreelakshmi Y, Sharma R (2014) Complex and shifting interactions of phytochromes regulate fruit development in tomato. *Plant Cell Environ* **37**: 1688–1702
- Guyer L, Hofstetter SS, Christ B, Lira BS, Rossi M, Hörtensteiner S (2014) Different mechanisms are responsible for chlorophyll dephytylation during fruit ripening and leaf senescence in tomato. *Plant Physiol* **166**: 44–56
- Hörtensteiner S (2013) Update on the biochemistry of chlorophyll breakdown. *Plant Mol Biol* **82**: 505–517
- Huang H, McLoughlin KE, Sorkin ML, Burgie ES, Bindbeutel RK, Vierstra RD, Nusinow DA (2019) PCH1 regulates light, temperature, and circadian signaling as a structural component of phytochrome B-photobodies in *Arabidopsis*. *Proc Natl Acad Sci USA* **116**: 8603–8608
- Inagaki N, Kinoshita K, Kagawa T, Tanaka A, Ueno O, Shimada H, Takano M (2015) Phytochrome B mediates the regulation of chlorophyll biosynthesis through transcriptional regulation of *ChlH* and *GUN4* in rice seedlings. *PLoS ONE* **10**: e0135408
- Ishida A, Toma T, Marjenah M (2000) Leaf gas exchange and canopy structure under wet and drought years in *Macaranga conifera*, a tropical pioneer tree. *Rainforest Ecosystems of East Kalimantan* **140**: 129–142
- Jung JH, Domijan M, Klose C, Biswas S, Ezer D, Gao M, Khattak AK, Box MS, Charoensawan V, Cortijo S, et al (2016) Phytochromes function as thermosensors in *Arabidopsis*. *Science* **354**: 886–889
- Karlova R, Rosin FM, Busscher-Lange J, Parapunova V, Do PT, Fernie AR, Fraser PD, Baxter C, Angenent GC, de Maagd RA (2011) Transcriptome and metabolite profiling show that APETALA2a is a major regulator of tomato fruit ripening. *Plant Cell* **23**: 923–941
- Kerckhoffs LHJ, Kelmenson PM, Schreuder MEL, Kendrick CI, Kendrick RE, Hanhart CJ, Koornneef M, Pratt LH, Cordonnier-Pratt MM (1999) Characterization of the gene encoding the apoprotein of phytochrome

- B2 in tomato, and identification of molecular lesions in two mutant alleles. *Mol Gen Genet* **261**: 901–907
- Kerckhoffs LHJ, Schreuder MEL, VanTuinen A, Koornneef M, Kendrick RE** (1997) Phytochrome control of anthocyanin biosynthesis in tomato seedlings: Analysis using photomorphogenic mutants. *Photochem Photobiol* **65**: 374–381
- Kerckhoffs LHJ, Van Tuinen A, Hauser BA, Cordonnier Pratt MM, Nagatani A, Koornneef M, Pratt LH, Kendrick RE** (1996) Molecular analysis of tri-mutant alleles in tomato indicates the Tri locus is the gene encoding the apoprotein of phytochrome B1. *Planta* **199**: 152–157
- Kim K, Jeong J, Kim J, Lee N, Kim ME, Lee S, Chang Kim S, Choi G** (2016) PIF1 regulates plastid development by repressing photosynthetic genes in the endodermis. *Mol Plant* **9**: 1415–1427
- Klee HJ, Giovannoni JJ** (2011) Genetics and control of tomato fruit ripening and quality attributes. *Annu Rev Genet* **45**: 41–59
- Koini MA, Alvey L, Allen T, Tilley CA, Harberd NP, Whitelam GC, Franklin KA** (2009) High temperature-mediated adaptations in plant architecture require the bHLH transcription factor PIF4. *Curr Biol* **19**: 408–413
- Lazarova GI, Kerckhoffs LHJ, Brandstätter J, Matsui M, Kendrick RE, Cordonnier-Pratt MM, Pratt LH** (1998a) Molecular analysis of *PHYA* in wild-type and phytochrome A-deficient mutants of tomato. *Plant J* **14**: 653–662
- Lazarova GI, Kubota T, Frances S, Peters JL, Hughes MJ, Brandstätter J, Széll M, Matsui M, Kendrick RE, Cordonnier-Pratt MM, et al** (1998b) Characterization of tomato *PHYB1* and identification of molecular defects in four mutant alleles. *Plant Mol Biol* **38**: 1137–1146
- Legris M, Klose C, Burgie ES, Rojas CCR, Neme M, Hiltbrunner A, Wigge PA, Schäfer E, Vierstra RD, Casal JJ** (2016) Phytochrome B integrates light and temperature signals in *Arabidopsis*. *Science* **354**: 897–900
- Legris M, Nieto C, Sellaro R, Prat S, Casal JJ** (2017) Perception and signalling of light and temperature cues in plants. *Plant J* **90**: 683–697
- Lira BS, de Setta N, Rosado D, Almeida J, Freschi L, Rossi M** (2014) Plant degreening: Evolution and expression of tomato (*Solanum lycopersicum*) dephytylation enzymes. *Gene* **546**: 359–366
- Lira BS, Gramegna G, Trench BA, Alves FRR, Silva EM, Silva GFF, Thirumalaikumar VP, Lupi ACD, Demarco D, Purgatto E, et al** (2017) Manipulation of a senescence-associated gene improves fleshy fruit yield. *Plant Physiol* **175**: 77–91
- Liu L, Shao Z, Zhang M, Wang Q** (2015) Regulation of carotenoid metabolism in tomato. *Mol Plant* **8**: 28–39
- Llorente B, D'Andrea L, Ruiz-Sola MA, Botterweg E, Pulido P, Andilla J, Loza-Alvarez P, Rodríguez-Concepción M** (2016) Tomato fruit carotenoid biosynthesis is adjusted to actual ripening progression by a light-dependent mechanism. *Plant J* **85**: 107–119
- Lorrain S, Allen T, Duek PD, Whitelam GC, Fankhauser C** (2008) Phytochrome-mediated inhibition of shade avoidance involves degradation of growth-promoting bHLH transcription factors. *Plant J* **53**: 312–323
- Ma D, Li X, Guo Y, Chu J, Fang S, Yan C, Noel JP, Liu H** (2016) Cryptochrome 1 interacts with PIF4 to regulate high temperature-mediated hypocotyl elongation in response to blue light. *Proc Natl Acad Sci USA* **113**: 224–229
- Martín G, Leivar P, Ludevid D, Tepperman JM, Quail PH, Monte E** (2016) Phytochrome and retrograde signalling pathways converge to antagonistically regulate a light-induced transcriptional network. *Nat Commun* **7**: 11431
- Martínez-García JF, Huq E, Quail PH** (2000) Direct targeting of light signals to a promoter element-bound transcription factor. *Science* **288**: 859–863
- Nakamura H, Muramatsu M, Hakata M, Ueno O, Nagamura Y, Hirochika H, Takano M, Ichikawa H** (2009) Ectopic overexpression of the transcription factor OsGLK1 induces chloroplast development in non-green rice cells. *Plant Cell Physiol* **50**: 1933–1949
- Nguyen CV, Vrebalov JT, Gapper NE, Zheng Y, Zhong S, Fei Z, Giovannoni JJ** (2014) Tomato GOLDEN2-LIKE transcription factors reveal molecular gradients that function during fruit development and ripening. *Plant Cell* **26**: 585–601
- Oh S, Montgomery BL** (2014) Phytochrome-dependent coordinate control of distinct aspects of nuclear and plastid gene expression during anterograde signaling and photomorphogenesis. *Front Plant Sci* **5**: 171
- Park E, Kim Y, Choi G** (2018) Phytochrome B requires PIF degradation and sequestration to induce light responses across a wide range of light conditions. *Plant Cell* **30**: 1277–1292
- Qiu Y, Li M, Kim RJ, Moore CM, Chen M** (2019) Daytime temperature is sensed by phytochrome B in *Arabidopsis* through a transcriptional activator HEMERA. *Nat Commun* **10**: 140
- Quadrana L, Almeida J, Otaiza SN, Duffy T, Corrêa da Silva JV, de Godoy F, Asís R, Bermúdez L, Fernie AR, Carrari F, et al** (2013) Transcriptional regulation of tocopherol biosynthesis in tomato. *Plant Mol Biol* **81**: 309–325
- Reynolds ES** (1963) The use of lead citrate at high pH as an electron-opaque stain in electron microscopy. *J Cell Biol* **17**: 208–212
- Rockwell NC, Su YS, Lagarias JC** (2006) Phytochrome structure and signaling mechanisms. *Annu Rev Plant Biol* **57**: 837–858
- Rosado D, Gramegna G, Cruz A, Lira BS, Freschi L, De Setta N, Rossi M** (2016) Phytochrome Interacting Factors (PIFs) in *Solanum lycopersicum*: Diversity, evolutionary history and expression profiling during different developmental processes. *PLoS ONE* **11**: e0165929
- Rosado D, Trench B, Bianchetti R, Zuccarelli R, Rodrigues Alves FR, Purgatto E, Segal Floh EI, Silveira Nogueira FT, Freschi L, Rossi M** (2019) Downregulation of PHYTOCHROME-INTERACTING FACTOR 4 influences plant development and fruit production. *Plant Physiol* **181**: 1360–1370
- Saidi Y, Finka A, Goloubinoff P** (2011) Heat perception and signalling in plants: A tortuous path to thermotolerance. *New Phytol* **190**: 556–565
- Sakuraba Y, Jeong J, Kang MY, Kim J, Paek NC, Choi G** (2014) Phytochrome-interacting transcription factors PIF4 and PIF5 induce leaf senescence in *Arabidopsis*. *Nat Commun* **5**: 4636
- Sharrock RA, Quail PH** (1989) Novel phytochrome sequences in *Arabidopsis thaliana*: Structure, evolution, and differential expression of a plant regulatory photoreceptor family. *Genes Dev* **3**: 1745–1757
- Sims DA, Gamon JA** (2003) Estimation of vegetation water content and photosynthetic tissue area from spectral reflectance: A comparison of indices based on liquid water and chlorophyll absorption features. *Remote Sens Environ* **84**: 526–537
- Song Y, Yang C, Gao S, Zhang W, Li L, Kuai B** (2014) Age-triggered and dark-induced leaf senescence require the bHLH transcription factors PIF3, 4, and 5. *Mol Plant* **7**: 1776–1787
- Spicher L, Almeida J, Gutbrod K, Pipitone R, Dörmann P, Glauser G, Rossi M, Kessler F** (2017) Essential role for phytyl kinase and tocopherol in tolerance to combined light and temperature stress in tomato. *J Exp Bot* **68**: 5845–5856
- Spicher L, Glauser G, Kessler F** (2016) Lipid antioxidant and galactolipid remodeling under temperature stress in tomato plants. *Front Plant Sci* **7**: 167
- Stephenson PG, Fankhauser C, Terry MJ** (2009) PIF3 is a repressor of chloroplast development. *Proc Natl Acad Sci USA* **106**: 7654–7659
- Suwa R, Hakata H, Hara H, El-Shemy HA, Adu-Gyamfi JJ, Nguyen NT, Kanai S, Lightfoot DA, Mohapatra PK, Fujita K** (2010) High temperature effects on photosynthate partitioning and sugar metabolism during ear expansion in maize (*Zea mays* L.) genotypes. *Plant Physiol Biochem* **48**: 124–130
- Takahashi S, Murata N** (2008) How do environmental stresses accelerate photoinhibition? *Trends Plant Sci* **13**: 178–182
- Toledo-Ortiz G, Johansson H, Lee KP, Bou-Torrent J, Stewart K, Steel G, Rodríguez-Concepción M, Halliday KJ** (2014) The HY5-PIF regulatory module coordinates light and temperature control of photosynthetic gene transcription. *PLoS Genet* **10**: e1004416
- Tomato Genome Consortium** (2012) The tomato genome sequence provides insights into fleshy fruit evolution. *Nature* **485**: 635–641
- van Eerden FJ, de Jong DH, de Vries AH, Wassenaar TA, Marrink SJ** (2015) Characterization of thylakoid lipid membranes from cyanobacteria and higher plants by molecular dynamics simulations. *Biochim Biophys Acta* **1848**: 1319–1330
- Velikova V, Várkonyi Z, Szabó M, Maslenkova L, Noguez I, Kovács L, Peeva V, Busheva M, Garab G, Sharkey TD, et al** (2011) Increased thermostability of thylakoid membranes in isoprene-emitting leaves probed with three biophysical techniques. *Plant Physiol* **157**: 905–916
- Watson ML** (1958) Staining of tissue sections for electron microscopy with heavy metals. II. Application of solutions containing lead and barium. *J Biophys Biochem Cytol* **4**: 727–730

- Wellburn A** (1994) The spectral determination of chlorophylls *a* and *b*, as well as total carotenoids, using various solvents with spectrophotometers of different resolution. *J Plant Physiol* **144**: 307–313
- Weller JL, Schreuder MEL, Smith H, Koornneef M, Kendrick RE** (2000) Physiological interactions of phytochromes A, B1 and B2 in the control of development in tomato. *Plant J* **24**: 345–356
- Yamori W, von Caemmerer S** (2009) Effect of Rubisco activase deficiency on the temperature response of CO₂ assimilation rate and Rubisco activation state: Insights from transgenic tobacco with reduced amounts of Rubisco activase. *Plant Physiol* **151**: 2073–2082
- Yuan XY, Wang RH, Zhao XD, Luo YB, Fu DQ** (2016) Role of the tomato Non-Ripening mutation in regulating fruit quality elucidated using iTRAQ protein profile analysis. *PLoS ONE* **11**: e0164335
- Zhang R, Sharkey TD** (2009) Photosynthetic electron transport and proton flux under moderate heat stress. *Photosynth Res* **100**: 29–43
- Zhang Y, Liu Z, Chen Y, He JX, Bi Y** (2015) PHYTOCHROME-INTERACTING FACTOR 5 (PIF5) positively regulates dark-induced senescence and chlorophyll degradation in *Arabidopsis*. *Plant Sci* **237**: 57–68
- Zhang Y, Mayba O, Pfeiffer A, Shi H, Tepperman JM, Speed TP, Quail PH** (2013) A quartet of PIF bHLH factors provides a transcriptionally centered signaling hub that regulates seedling morphogenesis through differential expression-patterning of shared target genes in *Arabidopsis*. *PLoS Genet* **9**: e1003244
- Zhao C, Liu B, Piao S, Wang X, Lobell DB, Huang Y, Huang M, Yao Y, Bassu S, Ciaia P, et al** (2017) Temperature increase reduces global yields of major crops in four independent estimates. *Proc Natl Acad Sci USA* **114**: 9326–9331
- Zhao F, Zhang D, Zhao Y, Wang W, Yang H, Tai F, Li C, Hu X** (2016) The difference of physiological and proteomic changes in maize leaves adaptation to drought, heat, and combined both stresses. *Front Plant Sci* **7**: 1471
- Zhou Y, Xun Q, Zhang D, Lv M, Ou Y, Li J** (2019) TCP transcription factors associate with PHYTOCHROME INTERACTING FACTOR 4 and CRYPTOCHROME 1 to regulate thermomorphogenesis in *Arabidopsis thaliana*. *iScience* **15**: 600–610